

Antonio Soria-Verdugo, Mariano Rubio-Rubio, Elke Goos, Uwe Riedel,
*Combining the lumped capacitance method and the simplified distributed
activation energy model to describe the pyrolysis of thermally small biomass
particles,*
Energy Conversion and Management 175 (2018) 164–172.

The original publication is available at www.elsevier.com

<https://doi.org/10.1016/j.enconman.2018.08.097>

© 2018. This manuscript version is made available under the CC-BY-NC-ND
4.0 license <http://creativecommons.org/licenses/by-nc-nd/4.0/>

**Combining the Lumped Capacitance Method and the simplified
Distributed Activation Energy Model to describe the pyrolysis of thermally
small biomass particles**

Antonio Soria-Verdugo^{a*}, Mariano Rubio-Rubio^b, Elke Goos^c, Uwe Riedel^c

^a *Carlos III University of Madrid (Spain), Energy Systems Engineering Group,
Thermal and Fluids Engineering Department. Avda. de la Universidad 30,
28911 Leganés (Madrid, Spain).*

^b *University of Jaén (Spain), Division of Fluid Mechanics, Department of
Mechanical and Mining Engineering. Campus de las Lagunillas, 23071 Jaén
(Spain).*

^c *Deutsches Zentrum für Luft- und Raumfahrt e.V. (German Aerospace Center,
DLR), Institute of Combustion Technology, Pfaffenwaldring 38-40, 70569
Stuttgart (Germany).*

* *corresponding author: asoria@ing.uc3m.es Tel: +34916248465.*

Abstract

The pyrolysis process of thermally small biomass particles was modeled combining the Lumped Capacitance Method (LCM) to describe the transient heat transfer and the Distributed Activation Energy Model (DAEM) to account for the chemical kinetics. The inverse exponential temperature increase predicted by the LCM was considered in the mathematical derivation of the DAEM, resulting in an Arrhenius equation valid to describe the evolution of the pyrolysis process under inverse exponential temperature profiles. The Arrhenius equation on which the simple LCM-DAEM model proposed is based was

derived for a wide range of pyrolysis reactor temperatures, considering the chemical kinetics data of four lignocellulosic biomass species: pine wood, olive kernel, thistle flower, and corncob. The LCM-DAEM model proposed was validated by comparison to the experimental results of the pyrolysis conversion evolution of biomass samples subjected to various inverse exponential temperature increases in a TGA. To extend the validation, additional biomass samples of *Chlorella Vulgaris* and sewage sludge were selected due to the different composition of microalgae and sludge compared to lignocellulosic biomass. The deviations obtained between the experimental measurements in TGA and the LCM-DAEM predictions for the evolution of the pyrolysis conversion, regarding the root mean square error of temperature, are below 5 °C in all cases. Therefore, the simple LCM-DAEM model proposed can describe accurately the pyrolysis process of a thermally small biomass particle, accounting for both the transient heat transfer and the chemical kinetics by solving a simple Arrhenius equation.

Keywords: Biomass pyrolysis; *Chlorella Vulgaris*; Distributed Activation Energy Model (DAEM); Inverse exponential temperature increase; Lumped Capacitance Method (LCM); Sewage sludge.

Nomenclature

- A Pre-exponential factor [s^{-1}].
- A_s Surface of the solid particle [m^2].
- α Pyrolysis conversion [%].
- Bi Biot number [-].
- β Heating rate [$^{\circ}C \text{ min}^{-1}$].

c	Heating parameter [min^{-1}].
c_s	Specific heat of the solid particle [$\text{J kg}^{-1} \text{K}^{-1}$].
d	Particle diameter [mm].
E	Activation energy [kJ mol^{-1}].
E_0	Mean value of gaussian distribution of activation energy [kJ mol^{-1}].
E_a	Value of activation energy for which the step function changes [kJ mol^{-1}].
ϕ_{ie}	Value of the ϕ -function for which the step function changes [-].
h	Convection coefficient [$\text{W m}^{-2} \text{K}^{-1}$].
k	Rate coefficient of a first-order reaction [s^{-1}].
k_s	Thermal conductivity of the solid particle [$\text{W m}^{-1} \text{K}^{-1}$].
L_c	Characteristic length [m].
ρ_s	Density of the solid particle [kg m^{-3}].
R	Universal gas constant [$\text{J mol}^{-1} \text{K}^{-1}$].
σ	Standard deviation of Gaussian distribution of activation energy [kJ mol^{-1}].
t	Time [min].
T	Temperature [$^{\circ}\text{C}$].
T_0	Ambient temperature [$^{\circ}\text{C}$].
T_{∞}	Reactor temperature [$^{\circ}\text{C}$].
V_s	Volume of the solid particle [m^3].

Abbreviations:

CV	Chlorella Vulgaris.
CFD	Computational Fluid Dynamics.
DAEM	Distributed Activation Energy Model.
HHV	High Heating Value.
LCM	Lumped Capacitance Method.

RMSE Root Mean Square Error.

SS Sewage Sludge.

TG Thermogravimetric.

TGA Thermogravimetric Analysis.

1. Introduction

Biomass is considered a promising substitute for fossil fuels due to its renewable character, worldwide availability, and globally neutral net CO₂ emissions, based on the carbon cycle. Biomass can be converted principally via biological or thermochemical processes (McKendry 2002). The biological conversion uses bacteria or enzymes to break the complex molecules of biomass into smaller molecules. However, this process is much slower than thermochemical conversion (Anca-Couce 2016). Thermochemical processing of biomass includes pyrolysis, combustion, gasification, hydrothermal liquefaction, and hydrothermal carbonization (Basu 2010). Among them, biomass pyrolysis, consisting in the thermal degradation of the solid fuel at a temperature ranging from 300 to 600 °C in the absence of oxygen, has some beneficial characteristics. Biomass pyrolysis is characterized by a low level of pollutant emissions derived from the conversion process, obtaining a liquid bio-oil as the primary product, which can be readily stored and transported, allowing its decentralized usage as a renewable fuel (Czernik and Bridgwater, 2004).

The design and optimization of biomass pyrolysis reactors are currently based on either Computational Fluid Dynamics (CFD) simulations or phenomenological models (Sharma et al., 2015), which require in both cases a detailed knowledge of the chemical kinetics of the thermal degradation reaction.

In this sense, several mathematical kinetic models are available in the literature, which can be classified into kinetic-fitting and kinetic-free models (Bach and Chen, 2017). The former involve the assumption for a functional form of the kinetic parameters, i.e., the activation energy and the pre-exponential factor. These fitting models include the single step model (Coats and Redfern, 1964), the sectional approach model (Lin et al., 2013), and the three pseudo-components model (Li et al., 2008). In contrast, kinetic-free models are based on experimental TGA measurements to calculate the activation energy and pre-exponential factor of the solid fuel pyrolysis reaction. The kinetic-free models comprise isoconversional models (Vyazovkin and Lesnicovich, 1992) and the simplified Distributed Activation Energy Model (DAEM) (Miura and Maki, 1998).

DAEM was developed initially by Vand (1943). The model was further simplified later by Miura (1995) and Miura and Maki (1998), resulting in a kinetic-free model known as simplified DAEM. Since then, this simplified DAEM has been widely used in the specific literature to describe the pyrolysis kinetics of a broad variety of solid fuels, including coal (Günes and Günes, 2008), charcoal (Várghegyi et al., 2002), polymers (Wanjun et al., 2005), lignocellulosic biomass (Sonobe and Worasuwanarak, 2008), microalgae (Ceylan and Kazan, 2015), sewage sludge (Soria-Verdugo et al., 2013), oil shale (Wang et al., 2009), and medical waste (Yan et al., 2009). The simplified DAEM has been proven to derive accurate results for the kinetic parameters of biomass pyrolysis from TGA measurements. However, its applicability estimating the evolution of the pyrolysis conversion with temperature is limited by the fact that simplified DAEM is valid exclusively for constant heating rates of the solid particles, i.e., linear increases of temperature with time. Nevertheless, the temperature increase of

solid particles in pyrolysis reactors is typically non-linear and, therefore, the direct application of the simplified DAEM in these reactors is not possible.

This paper deals with the limitation of the simplified DAEM to constant heating rates and is devoted to overcoming this limit. A simple model is proposed to describe the pyrolysis of thermally small particles, combining the Lumped Capacitance Method (LCM), to estimate the transient heat transfer of the solid particles, and the simplified Distributed Activation Energy Model (DAEM), to account for the chemical kinetics of the thermal degradation. The proposed LCM-DAEM model is based on an Arrhenius equation obtained following the mathematical procedure proposed by Miura (1995) and Miura and Maki (1998) for the simplified DAEM, but considering the inverse exponential temperature increase to which thermally small particles are subjected according to the LCM. The new Arrhenius equation for the LCM-DAEM was derived as a function of the reactor temperature, considering the pyrolysis kinetic data of several lignocellulosic biomass species. Finally, the validity of the Arrhenius equations derived was validated comparing the estimation of the pyrolysis conversion evolution predicted by the proposed LCM-DAEM model to experimental pyrolysis measurements of microalgae and sewage sludge, conducted in a thermogravimetric analyzer (TGA) under various inverse exponential temperature increases.

2. Theoretical Model

Pyrolysis of solid fuels is a complex process which involves both heat transfer and chemical reactions. In this regard, a simplified model is proposed to describe the pyrolysis reactions of small biomass particles. The model proposed

is based on combining the Lumped Capacitance Method to consider heat transfer between the environment and the solid particle with the simplified Distributed Activation Energy Model to account for the chemical kinetics of the pyrolysis reactions.

2.1. Lumped Capacitance Method (LCM)

When a biomass particle is fed to a reactor at a high temperature T_∞ , transient conduction occurs inside the particle, whose temperature increases with time. If the temperature inside the particle can be considered spatially uniform, a single temperature T can be employed to describe the time evolution of heat transfer between the reactor and the particle. This assumption is the base of the widely known Lumped Capacitance Method, for which the temperature of the particle can be determined by formulating a global energy balance on the particle, relating the convection heat transfer rate at the particle surface with the rate of change of internal energy of the particle:

$$h \cdot A_s \cdot (T_\infty - T) = \rho_s \cdot V_s \cdot c_s \frac{dT}{dt}, \quad (1)$$

where h is the convection coefficient, T_∞ is the reactor temperature, T is the temperature inside the particle, t is time, and A_s , V_s , ρ_s , and c_s are the solid particle surface, volume, density, and specific heat, respectively.

Integrating Eq. (1), considering the initial temperature of the solid particle T_0 when the particle is fed to the reactor, i.e., at the initial time $t = 0$, the time evolution of the particle temperature is obtained as an inverse exponential approximation to the reactor temperature T_∞ :

$$T = T_{\infty} - (T_{\infty} - T_0) \cdot \exp\left(-\frac{h \cdot A_s}{\rho_s \cdot V_s \cdot c_s} t\right). \quad (2)$$

The time-coefficient in the exponential function in Eq. (2) can be defined as the heating parameter:

$$c = \frac{h \cdot A_s}{\rho_s \cdot V_s \cdot c_s}, \quad (3)$$

which is constant for a specific biomass type, i.e., fixed values of A_s , V_s , ρ_s , and c_s , and reactor operating conditions, i.e., uniform value for h .

The essence of the LCM is the assumption of uniform spatial temperature distribution inside the solid particle during the transient heating process. Therefore, the validity of the LCM and, thus, of Eq. (2) to describe the temperature evolution of biomass particles, should be discussed in the light of that hypothesis. In that sense, the Biot number Bi is defined for transient conduction problems as the ratio of the thermal resistance by conduction inside the solid particle and the thermal resistance by convection at the particle surface, obtaining:

$$Bi = \frac{h \cdot L_c}{k_s}, \quad (4)$$

where h is the convection coefficient, k_s is the thermal conductivity of the solid particle, and L_c is the characteristic length, defined as the ratio between the solid particle volume V_s and its surface A_s .

Therefore, if $Bi \ll 1$, the thermal resistance by conduction inside the solid particle is negligible compared to the thermal resistance by convection at its

surface. Thus, the assumption of spatially uniform temperature is reasonable for cases with $Bi \ll 1$. In practice, the validity criterion for the central assumption of the LCM is $Bi \leq 0.1$, and a low error associated to the LCM can be expected when this validity criterion is satisfied (Incropera et al., 2007). The particles for which this criterion is met are called thermally small particles.

Assuming a spherical shape for the solid particles, the characteristic length can be related to the particle diameter d as $L_c = d/6$. In the case of biomass particles heated up in a reactor, typical values for the convection coefficient are $h \sim 20$ W/m²K, and thermal conductivity is approximately $k_s \sim 0.1$ W/m·K, and therefore the validity criterion for the LCM is satisfied provided that the particle diameter is $d \leq 3$ mm. In conclusion, the LCM can be used to estimate the particle temperature increase for small size biomass particles, such as short straws or olive stones, which are typically obtained fragmented as a residue of the olive oil industry (Pattara et al., 2010). In contrast, for those cases in which $Bi > 0.1$, appreciable temperature differences within these bigger solid particles exist. Then, spatial effects should be considered, and the heat equation must be solved to determine the temperature distribution inside these bigger particles.

2.2. Distributed Activation Energy Model (DAEM)

The simplified Distributed Activation Energy Model is widely used to describe the chemical kinetics of solid fuels pyrolysis. DAEM considers the solid fuel as a complex mixture of components, which decompose as a result of a large number of independent irreversible first-order reactions, with different associated activation energies, occurring either simultaneously or

consecutively. The conversion α during the pyrolysis reaction can be determined as follows:

$$1 - \alpha = \int_0^{\infty} \exp\left(-A \int_0^t e^{E/RT} dt\right) f(E) \cdot dE, \quad (5)$$

where α is the pyrolysis conversion at time t , A is the pre-exponential factor, E is the activation energy, R is the universal gas constant, T is the temperature, and $f(E)$ is the probability density function of the activation energy. The exponential term in Eq. (5) is the so-called ϕ function:

$$\phi = \exp\left(-A \int_0^t e^{-E/RT} dt\right). \quad (6)$$

Considering a constant heating rate β , i.e., a linear temperature increase $T = \beta \cdot t$, the time integral in the ϕ function is converted to a temperature integral, which can be simplified using the approximation of Coats and Redfern (1964) as follows:

$$\phi = \exp\left(-\frac{A}{\beta} \int_0^T e^{-E/RT} dT\right) \approx \exp\left(-\frac{ART^2}{\beta E} e^{-E/RT}\right). \quad (7)$$

This expression for the ϕ function can be approximated as a step function at a value of the activation energy of $E = E_a$, obtaining the following expression for the pyrolysis conversion α , taking into account the normalization criterion for the probability density function of activation energies $f(E)$:

$$\alpha = 1 - \int_{E_a}^{\infty} f(E) \cdot dE = \int_0^{E_a} f(E) \cdot dE. \quad (8)$$

The value of the ϕ function for which the step function changes, i.e., the value of ϕ for $E = E_a$, should be established. Miura (1995) proposed a value of $\phi(E_a) = 0.58$, which was found to be valid for a broad variety of biomass samples. Therefore, using this value for the ϕ function, and taking the logarithm to Eq. (7), the Arrhenius equation for the simplified DAEM is obtained:

$$\ln\left(\frac{\beta}{T^2}\right) = \ln\left(\frac{AR}{E}\right) + 0.6075 - \frac{E}{RT}. \quad (9)$$

Considering this Arrhenius equation, Miura and Maki (1998) proposed a procedure to determine the activation energy E and the pre-exponential factor A of the pyrolysis reaction based on thermogravimetric pyrolysis measurements conducted for various heating rates β .

However, the main limitation of this widely used simplified DAEM is its restriction to constant heating rates, i.e., linear increases of temperature with time. To avoid this limitation, the mathematical procedure of simplified DAEM was modified by Soria-Verdugo et al. (2016) to derive Arrhenius equations for parabolic and positive exponential temperature increases. Nevertheless, no Arrhenius equation available in the literature can describe the pyrolysis kinetics under inverse exponential temperature increases, such as those predicted by the LCM, Eq. (2). In this regard, the following subsection presents the mathematical derivation of an Arrhenius equation, based on the simplified DAEM, valid for inverse exponential temperature increases of the solid particles, as modeled by the LCM.

2.3. Combined LCM and simplified DAEM (LCM-DAEM)

The pyrolysis of thermally small particles, i.e., $Bi < 0.1$, can be modeled by combining the LCM to characterize the transient heat transfer and the simplified DAEM to describe the chemical kinetics. Deriving the inverse exponential temperature increase predicted by the LCM, Eq. (2), the time variation can be related to the temperature variation as follows:

$$dt = \frac{dT}{c(T_{\infty} - T)}. \quad (10)$$

Therefore, the time integral in the ϕ function, Eq. (6), can be converted to a temperature integral, considering an inverse exponential temperature increase, using Eq. (10):

$$\phi = \exp\left(-\frac{A}{c} \int_0^T \frac{e^{-E/RT}}{T_{\infty} - T} dT\right). \quad (11)$$

The temperature integral in Eq. (11) can be rewritten, using a substitution method, in terms of a new pair of variables, $z = E/(RT)$ and $z_{\infty} = E/(RT_{\infty})$:

$$\int_0^T \frac{e^{-E/RT}}{T_{\infty} - T} dT = \int_z^{\infty} \frac{z_{\infty} e^{-z}}{z(z - z_{\infty})} dz. \quad (12)$$

The solution to this integral is:

$$\int_z^{\infty} \frac{z_{\infty} e^{-z}}{z(z - z_{\infty})} dz = e^{-z_{\infty}} \text{Ei}(z - z_{\infty}) - \text{Ei}(z), \quad (13)$$

where $\text{Ei}(z)$ is the exponential integral, which can be approximated to (Bleistein and Handelsman, 1987):

$$\text{Ei}(z) = \frac{e^{-z}}{z} \sum_{n=0}^{\infty} \frac{n!}{(-z)^n}, \quad (14)$$

and therefore:

$$\text{Ei}(z - z_{\infty}) = \frac{e^{-(z-z_{\infty})}}{z - z_{\infty}} \sum_{n=0}^{\infty} \frac{n!}{(-z + z_{\infty})^n}, \quad (15)$$

Thus, considering these approximations for the exponential integrals, Eq. (13) can be expressed as follows:

$$\int_z^{\infty} \frac{z_{\infty} e^{-z}}{z(z - z_{\infty})} dz = e^{-z} \sum_{n=1}^{\infty} (-1)^{n-1} (n-1)! \left[(z - z_{\infty})^{-n} - z^{-n} \right], \quad (16)$$

which, in terms of the original variables, provides an approximation to the temperature integral in Eq. (11) that reads:

$$\int_0^T \frac{e^{-E/RT}}{T_{\infty} - T} dT = e^{-E/RT} \sum_{n=1}^{\infty} (-1)^{n-1} (n-1)! \left(\frac{R}{E} \right)^n \left[\left(\frac{T \cdot T_{\infty}}{T_{\infty} - T} \right)^n - T^n \right]. \quad (17)$$

Considering typical values of the activation energy of biomass pyrolysis of $E \sim 200$ kJ/mol, biomass pyrolysis temperature of $T \sim 300$ °C, and the universal gas constant $R = 8.314$ J/mol, a low error would be committed by approximating the temperature integral to the first term ($n = 1$) in Eq. (17), provided that the reactor temperature is around 250 °C above the characteristic temperature of biomass pyrolysis, i.e., $T_{\infty} - T > 250$ °C. Considering this approximation for the temperature integral, the ϕ function, Eq. (11), yields:

$$\phi \approx \exp\left(-\frac{ART^2}{cE(T_{\infty} - T)} \right). \quad (18)$$

Following the same mathematical procedure as for the original simplified DAEM, valid only for linear temperature increases, the exponential expression of the ϕ function obtained for inverse exponential temperature increases, Eq. (18), is approximated to a step function changing at an activation energy $E = E_a$. Then, according to Eq. (5), the pyrolysis conversion α can be written as follows:

$$\alpha = 1 - \int_0^{\infty} \phi \cdot f(E) \cdot dE = 1 - \int_{E_a}^{\infty} f(E) \cdot dE = \int_0^{E_a} f(E) \cdot dE. \quad (19)$$

Thus, the value of the activation energy for which the step function changes, $E = E_a$, can be determined satisfying the second equality in Eq. (19), that is:

$$\int_0^{\infty} \phi \cdot f(E) \cdot dE = \int_{E_a}^{\infty} f(E) \cdot dE, \quad (20)$$

and, once this activation energy E_a is obtained, the value of the ϕ function $\phi(E_a) = \phi_e$ is determined substituting in Eq. (11). To determine the activation energy E_a from Eq. (20), a statistical distribution needs to be assumed for $f(E)$, with the Gaussian distribution being the most typical assumption (Cai and Liu, 2008; Cai et al., 2014):

$$f(E) = \frac{1}{\sigma\sqrt{2\pi}} \exp\left(-\frac{(E-E_0)^2}{2\sigma^2}\right), \quad (21)$$

where E_0 is the mean and σ the standard deviation of the activation energy probability distribution.

The procedure to determine E_a from the fulfilment of Eq. (20) was followed by Miura (1995), using various biomass samples, to determine the proper value of the ϕ function for linear temperature increases, obtaining a value of $\phi(E_a) =$

0.58. This procedure was also followed in a previous work by Soria-Verdugo et al. (2016) to determine the values of $\phi(E_a)$ for both parabolic and positive exponential temperature increases. In this previous work, the pyrolysis chemical kinetic data of four lignocellulosic biomasses were employed to calculate the proper values of $\phi(E_a)$, obtaining reliable values. Therefore, the calculation of the ϕ function value for inverse exponential temperature increases $\phi(E_a) = \phi_e$ will also be based on the same kinetic data of pine wood, olive kernel, thistle flower, and corncob as in Soria-Verdugo et al. (2016). This kinetic data, included in Table 1, were obtained for the distributions of activation energy and pre-exponential factor as a function of the pyrolysis conversion reported in Soria-Verdugo et al. (2015).

Table 1. Pyrolysis kinetic data of various lignocellulosic biomass species.

Sample	E_0 [kJ/mol]	σ [kJ/mol]	A [s⁻¹]
Pine wood	165.0	2.6	$1.57 \cdot 10^{12}$
Olive kernel	162.2	3.2	$4.11 \cdot 10^{12}$
Thistle flower	154.5	1.6	$2.80 \cdot 10^{11}$
Corn cob	183.5	5.0	$2.31 \cdot 10^{14}$

Using the mean E_0 and standard deviation σ of the activation energy, the probability distribution $f(E)$ can be built using Eq. (21), and the value of the activation energy E_a for which the ϕ function changes can be obtained from satisfying Eq. (20). Once the value of E_a is obtained, the value of $\phi(E_a) = \phi_e$ can be calculated from Eq. (18). However, for inverse exponential temperature increases as those predicted by the LCM, since the ϕ function obtained, Eq. (18), depends on the reactor temperature T_∞ , the value of $\phi(E_a) = \phi_e$ is also

expected to be a function of this reactor temperature. Therefore, the process proposed by Miura (1995) to determine $\phi(E_a)$ will be followed for various reactor temperatures, to determine the dependence of ϕ_e on T_∞ .

As an example, the process to determine ϕ_e is shown graphically in Figure 1 for pine wood at $T_\infty = 550$ °C and $T_\infty = 650$ °C. First, using the kinetic data included in Table 1, the probability density function of the activation energy $f(E)$ is built employing Eq. (21). Secondly, the approximation of the ϕ function, Eq. (18), is used to determine the curve $\phi \cdot f(E)$. Then, the value of E_a is determined as the activation energy for which Eq. (20) is satisfied, i.e., the area under the curve of $f(E)$ from this activation energy E_a to infinity equals the whole area under the curve $\phi \cdot f(E)$. Finally, using the simplification of the ϕ function, Eq. (18), the value of the ϕ function for this activation energy is obtained $\phi(E_a) = \phi_e$. Figure 1 shows that, as expected, the value of ϕ_e is a function of T_∞ , due to the dependence of the ϕ function on the reactor temperature. For a reactor temperature of $T_\infty = 550$ °C, the value obtained for the ϕ function is $\phi_e = 0.482$, whereas for a temperature of $T_\infty = 650$ °C this value is $\phi_e = 0.550$. Similar results to those shown in Figure 1 for pine wood were obtained for the other three lignocellulosic biomass species considered (olive kernel, thistle flower, and corncob) resulting in similar values of ϕ_e , thus, these results are not shown graphically to avoid repetition. In the plots of the ϕ function included in Figure 1, a sharp variation of ϕ can be observed in the typical range of activation energies for biomass pyrolysis, from 100 to 250 kJ/mol, which justifies the simplification of considering the ϕ function as a step function.

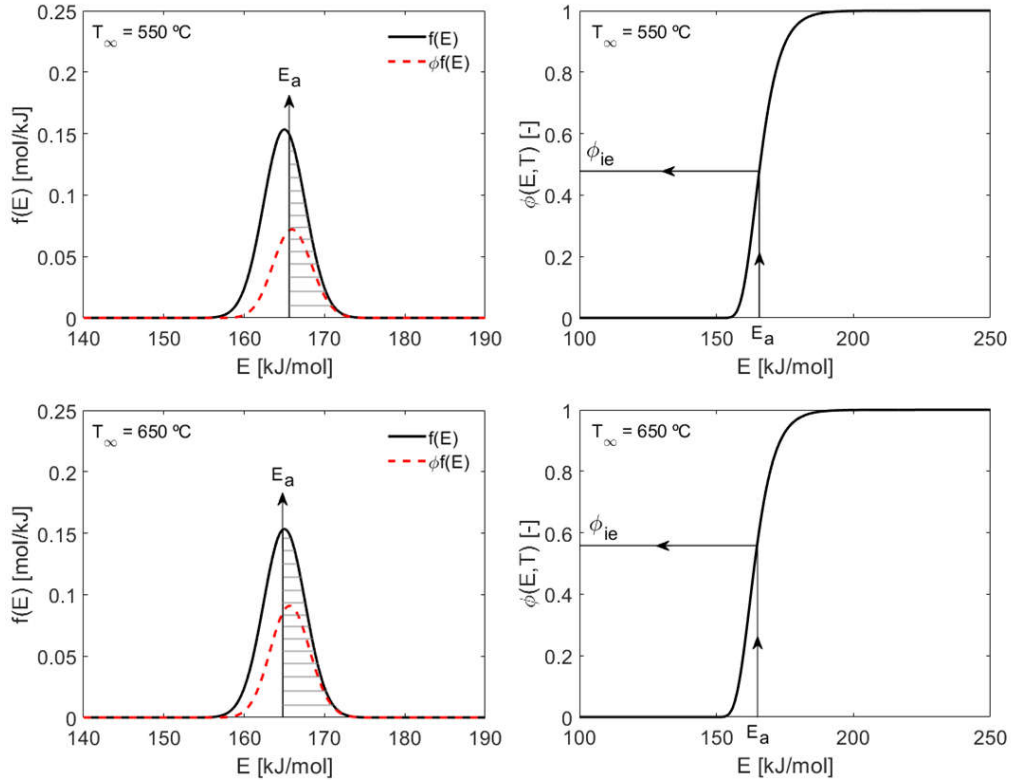


Figure 1. Process to determine ϕ_{ie} .

To determine the dependence of ϕ_{ie} on T_{∞} , the procedure described in Figure 1 was repeated for each lignocellulosic sample included in Table 1, varying the reactor temperature T_{∞} from 450 to 750 °C in intervals of 10 °C. Similar values of ϕ_{ie} were obtained for the different samples for each reactor temperature. Therefore, the values of ϕ_{ie} determined for each biomass specie were averaged to obtain the dependence of ϕ_{ie} on T_{∞} . The averaged values of ϕ_{ie} are depicted in Figure 2 as a function of the reactor temperature T_{∞} , together with a parabolic fitting of the values obtained. The parabolic fitting of ϕ_{ie} with T_{∞} , shown in Figure 2, follows the equation:

$$\phi_{ie} = -1.533 \cdot 10^{-6} \cdot T_{\infty}^2 + 2.577 \cdot 10^{-3} \cdot T_{\infty} - 0.4745, \quad (22)$$

with T_∞ in °C. This parabolic relation describes accurately the dependence of ϕ_e on T_∞ , obtaining a determination coefficient R^2 for the fitting higher than 0.99.

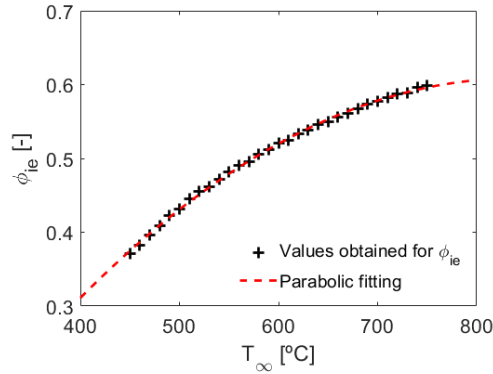


Figure 2. Values obtained for ϕ_e as a function of the reactor temperature T_∞ (black +) and parabolic fitting (red dashed line).

The value of ϕ_e can be used in the simplification of the ϕ function, Eq. (18), to derive the Arrhenius equation for inverse exponential temperature increases. By taking the logarithm twice and rearranging terms, the following expression is obtained:

$$\ln\left(\frac{c(T_\infty - T)}{T^2}\right) = \ln\left(\frac{AR}{E}\right) - \ln(-\ln(\phi_e)) - \frac{E}{R} \frac{1}{T} \quad (23)$$

Therefore, using Eq. (22) to calculate the value of ϕ_e as a function of the reactor temperature T_∞ , an Arrhenius equation can be derived for a specific reactor temperature. For instance, for thermally small biomass particles in reactors at temperatures of 550 °C and 650 °C, the Arrhenius equations that describe the pyrolysis process read:

$$\ln\left(\frac{c(T_\infty - T)}{T^2}\right) = \ln\left(\frac{AR}{E}\right) + 0.3070 - \frac{E}{R} \frac{1}{T}, \quad \text{for } T_\infty = 550 \text{ °C} \quad (24)$$

$$\ln\left(\frac{c(T_{\infty} - T)}{T^2}\right) = \ln\left(\frac{AR}{E}\right) + 0.5233 - \frac{E}{R} \frac{1}{T}, \quad \text{for } T_{\infty} = 650 \text{ }^{\circ}\text{C} \quad (25)$$

These simple Arrhenius equations describe the whole pyrolysis process of thermally small biomass particles when they are fed to a reactor at a higher temperature T_{∞} . Thus, provided that the pyrolysis kinetic parameters, i.e., E and A , of the biomass employed are known as a function of the pyrolysis conversion α , and that the heating parameter c , Eq. (3), is estimated, the calculation of the temperature for which each conversion occurs can be carried out by solving the transcendental Arrhenius equation for specific values of the pyrolysis conversion. Therefore, an estimation of the mass released during the pyrolysis of thermally small biomass particles as a function of temperature or time, considering Eq. (2), can be made by solving the Arrhenius equation corresponding to the reactor temperature employed (see Eq. (24) or Eq. (25)). The calculations were done with units of K and s for temperature and time, respectively, to be in agreement with the international system of units. However, to increase the readability of the paper, temperature values were reported in $^{\circ}\text{C}$ and time in min, and consequently, the heating rates and heating parameters were reported in K/min and min^{-1} , respectively.

Since the proposed LCM-DAEM model combines the LCM to describe the transient heat transfer problem and simplified DAEM to account for the chemical kinetics of the biomass pyrolysis process, it is subjected to the limitations of both methods. Therefore, the maximum size of the particles for which the proposed model is valid is limited, and must satisfy the condition of $\text{Bi} \leq 0.1$, and the pyrolysis reactions are assumed to follow all first-order kinetics, which is a general hypothesis of DAEM. In addition, the heating parameter c was

considered to be constant during the derivation of the LCM-DAEM model. However, the variables affecting the heating parameter c , Eq. (3), might be subjected to changes during the biomass pyrolysis, although the range of variation of these variables would be restricted by the limited size of the particles imposed by the LCM. Thus, considering a constant value of c for the derivation of the model is a reasonable assumption. Nevertheless, if information about the variation of the heating parameter c , or its affecting parameters, is available, the LCM-DAEM model could be modified to account also for variations of c .

3. Materials and Methods

3.1. Thermogravimetric Analyzer

The pyrolysis measurements were conducted in a thermogravimetric analyzer TGA Q500 from TA Instruments. The inert atmosphere required for pyrolysis conditions was guaranteed by supplying a flow rate of 60 ml/min of nitrogen 3.0 to the furnace. A small mass of the sample of 10.0 ± 0.5 mg, composed of particles under $100 \mu\text{m}$, was employed for the tests to limit heat and mass transfer effects inside the sample. Thus, using this small sample size, the temperature of the sample is assumed to be that imposed by the TGA furnace, which in this case will be inverse exponential temperature increases as those predicted by the LCM. Considering the sensitivity of the TGA mass measurement of $0.1 \mu\text{g}$ and the weighing precision of $\pm 0.01\%$, the sample mass used provides a high signal-to-noise ratio.

To check the validity of the proposed LCM-DAEM model using TGA pyrolysis measurements, inverse exponential temperature increases as those predicted by the LCM, Eq. (2), should be programmed to the TGA. However, the TGA

permits only constant heating rates, i.e., linear increases in temperature with time. Therefore, the inverse exponential temperature profiles required were built from a series of 25 constant heating rates, as described in Soria-Verdugo et al. (2016) for parabolic and positive exponential temperature increases. Two different inverse exponential temperature increases, corresponding to heating parameters of $c = 0.06 \text{ min}^{-1}$ and $c = 0.18 \text{ min}^{-1}$, were built to heat the samples in the TGA furnace up to two different temperatures of $T_{\infty} = 550 \text{ }^{\circ}\text{C}$ and $T_{\infty} = 650 \text{ }^{\circ}\text{C}$. The heating parameters tested were selected to limit the values of the 25 constant heating rates composing the inverse exponential temperature profiles to operative values for the TGA employed. For the two heating parameters and reactor temperatures selected, the constant heating rates required to build the temperature profiles range between $0.03 \text{ }^{\circ}\text{C}/\text{min}$ and $100 \text{ }^{\circ}\text{C}/\text{min}$, values that can be handled in the TGA Q500 used. In fact, heating rates up to $200 \text{ }^{\circ}\text{C}/\text{min}$ can be programmed in this equipment (Soria-Verdugo et al., 2014). A blank experiment was also conducted for each heating parameter and reactor temperature to subtract buoyancy effects, and the repeatability of the pyrolysis tests was checked by repeating each run three times, obtaining relative discrepancies lower than 0.5%.

3.2. Biomass Characterization

The derivation of the Arrhenius equation for the LCM-DAEM model proposed was based on the ϕ_{ie} values obtained from the pyrolysis kinetics data of four lignocellulosic biomass species, typically composed of hemicellulose, cellulose, lignin, and low amounts of inorganic matter. Therefore, the validation of the model was performed by comparing TGA pyrolysis measurements of non-lignocellulosic biomass samples to the predictions of the model, to prove the

validity of the proposed equations for a broad range of biomass types. In this regard, biomass samples of microalgae, which are composed of carbohydrates, proteins, lipids, and other minor components, and sewage sludge (SS), which comprises organic and inorganic matter, were analyzed. Among the different microalgae species, *Chlorella Vulgaris* (CV) was selected since it is widely grown and used (Figueira et al., 2015).

The basic characterization of the microalgae and sewage sludge tested are shown in Table 2. The characterization consists in a proximate analysis, performed in the TGA Q500 from TA Instruments, an ultimate analysis, carried out in a LECO TruSpec CHN Macro and TruSpec S analyzer, and a heating value test, conducted in a Parr 6300 isoperibolic calorimeter. The results for the *Chlorella Vulgaris* sample were reported in Soria-Verdugo et al. (2018), whereas the sewage sludge results were taken from Soria-Verdugo et al. (2017a). However, in the case of the sewage sludge, the sulfur content was measured in the LECO TruSpec S analyzer to include the complete data in Table 2.

Table 2. Results of the basic characterization of *Chlorella Vulgaris* and sewage sludge (PA: Proximate Analysis, UA: Ultimate Analysis, VM: Volatile Matter, A: Ash, C: Carbon, H: Hydrogen, N: Nitrogen, S: Sulfur, O: Oxygen, HHV: High Heating Value, db: dry basis, daf: dried ash free basis, * calculated by difference).

	PA [%db]		UA [%daf]					HHV [db]
	VM	A	C	H	N	S	O*	[MJ/kg]
Chlorella Vulgaris	76.26	13.11	59.06	8.81	11.39	0.66	20.08	21.57
Sewage Sludge	57.11	34.66	56.46	7.91	8.42	2.83	24.38	15.73

A detailed comparison of the results obtained from the basic characterization of *Chlorella Vulgaris* and sewage sludge was carried out in a previous work (Soria-Verdugo et al., 2017b), where these results were found to be similar to those reported in the literature by several authors.

4. Results and Discussion

4.1. TGA measurements

The capability of the TGA to reproduce inverse exponential temperature increases as a combination of a series of 25 linear temperature increases was checked. Figure 3 shows the time evolution of temperature measured by the TGA for the two final reactor temperatures of $T_{\infty} = 550$ °C and $T_{\infty} = 650$ °C and the two inverse exponential temperature profiles, with heating parameters $c = 0.06$ min⁻¹ and $c = 0.18$ min⁻¹, tested. Despite the fact that the curves are composed of 25 constant heating rates, the inverse exponential form of the temperature profiles measured by the TGA is smooth. The measured temperature increases are depicted in Figure 3, and the fitting of these data to inverse exponential increases in the form of Eq. (2) resulted in determination coefficients $R^2 > 0.999$ in all cases. Therefore, the series of linear heating steps programmed to the TGA accurately describes the inverse exponential temperature increases required to validate the proposed LCM-DAEM model.

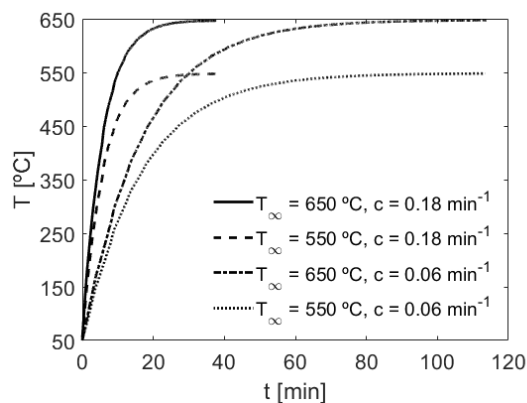


Figure 3. Temperature profiles measured in the TGA for different reactor temperatures and heating parameters.

The TGA inverse exponential temperature profiles shown in Figure 3 were employed to conduct pyrolysis tests using *Chlorella Vulgaris* and sewage sludge samples. The TG curves obtained, depicting the time evolution of the pyrolysis conversion α , are represented in Figure 4 for both samples. Clear differences are observed for the pyrolysis tests conducted for different inverse exponential heating parameters. A faster pyrolysis process occurs for the tests at $c = 0.18 \text{ min}^{-1}$ which last around 10 min, in contrast to the approximately 50 min required by the pyrolysis experiments at $c = 0.06 \text{ min}^{-1}$. There are also differences between the TG curves corresponding to the same heating parameter and different reactor temperatures due to the faster heating process required to attain a higher temperature following the same inverse exponential temperature curve. Similar TG curves were obtained for *Chlorella Vulgaris* and sewage sludge, characterized in both cases by steep increases of the pyrolysis conversion with time, as a consequence of the vigorous release of volatile matter, especially for the faster heating, $c = 0.18 \text{ min}^{-1}$. However, Figure 4 shows also differences for the TG curves of *Chlorella Vulgaris* and sewage sludge for the lower heating parameter of $c = 0.06 \text{ min}^{-1}$ tested. In these cases,

the solid residue generated after the release of highly volatile matter contained in sewage sludge, during around 20 min, seems to react as time progresses, resulting in a slight increase of the conversion with time during the final part of the pyrolysis test, $t > 20$ min. In contrast, this effect was less pronounced for the *Chlorella Vulgaris* sample.

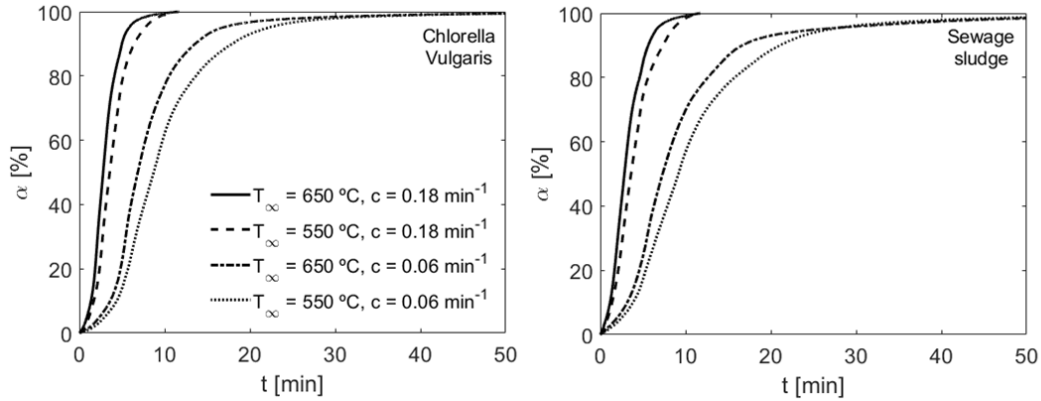


Figure 4. Pyrolysis conversion curves for *Chlorella Vulgaris* and sewage sludge.

4.2. Validation of the LCM-DAEM model proposed

The validation of the proposed LCM-DAEM model was based on the comparison of the pyrolysis conversion measured in TGA with the predictions of the model for both *Chlorella Vulgaris* and sewage sludge pyrolysis. This comparison was carried out for reactor temperatures of $T_\infty = 550$ °C and $T_\infty = 650$ °C and for the two inverse exponential temperature profiles tested, corresponding to heating parameters of $c = 0.06$ min⁻¹ and $c = 0.18$ min⁻¹. The prediction of the LCM-DAEM model is obtained by solving the corresponding Arrhenius equation, i.e., Eq. (24) for $T_\infty = 550$ °C and Eq. (25) for $T_\infty = 650$ °C, to determine the temperature of the sample T for specific values of the pyrolysis conversion α . To that end, the evolution of the pre-exponential factor A and the activation energy E of the biomass sample with the pyrolysis conversion α

should be known. The evolution of A and E of *Chlorella Vulgaris* and sewage sludge with the pyrolysis conversion α , for a range between 5% and 95% with intervals of 1%, was reported in Soria-Verdugo et al. (2017b), and they can also be observed in the supplementary material of this paper. These evolutions of the pre-exponential factor A and activation energy E with the pyrolysis conversion α were obtained by applying the simplified DAEM to TGA pyrolysis measurements conducted using nine different constant heating rates.

The kinetic parameters of the pyrolysis reactions A and E reported in Soria-Verdugo et al. (2017b) were introduced in the transcendental Arrhenius equations, Eq. (24) for $T_\infty = 550$ °C and Eq. (25) for $T_\infty = 650$ °C. These Arrhenius equations have no analytical solution; thus, they should be solved using some simple numerical method such as the Newton-Raphson technique. The Arrhenius equations were numerically solved for values of the pyrolysis conversion α between 5% and 95% varying with intervals of 1%. The estimation of the temperature T in the whole range of pyrolysis conversion α was determined, for both *Chlorella Vulgaris* and sewage sludge, for pyrolysis reactor temperatures of $T_\infty = 550$ °C and $T_\infty = 650$ °C, using the two inverse exponential temperature profiles measured experimentally in TGA (heating parameters of $c = 0.06$ min⁻¹ and $c = 0.18$ min⁻¹) in the Arrhenius equations. Therefore, the complex combined heat transfer and chemical kinetics problem of biomass pyrolysis is simplified with the proposed LCM-DAEM model to solve a simple Arrhenius equation.

The predictions obtained from the proposed LCM-DAEM model for the evolution of pyrolysis conversion α with temperature T were compared with the

experimental measurements performed in TGA. As an example, Figure 5 represents the $\alpha - T$ curves measured in TGA together with the LDM-DAEM model estimations for the pyrolysis of both *Chlorella Vulgaris* and sewage sludge for the case of the lower reactor temperature and heating parameter, $T_\infty = 550 \text{ }^\circ\text{C}$ and $c = 0.06 \text{ min}^{-1}$. The experimental curves of α versus T are obtained directly from the pyrolysis conversion curves shown in Figure 4, considering the temperature profile imposed by the TGA to convert time into temperature. The numerical results obtained from the LCM-DAEM model for the evolution of the pyrolysis conversion α with temperature T , obtained solving the corresponding Arrhenius equation and depicted in Figure 5 for a pyrolysis conversion range between 5% and 95% in intervals of 1%, are in good agreement with the experimental measurements carried out in TGA for both *Chlorella Vulgaris* and sewage sludge, even though these two biomass samples have a totally different composition compared to lignocellulosic biomass.

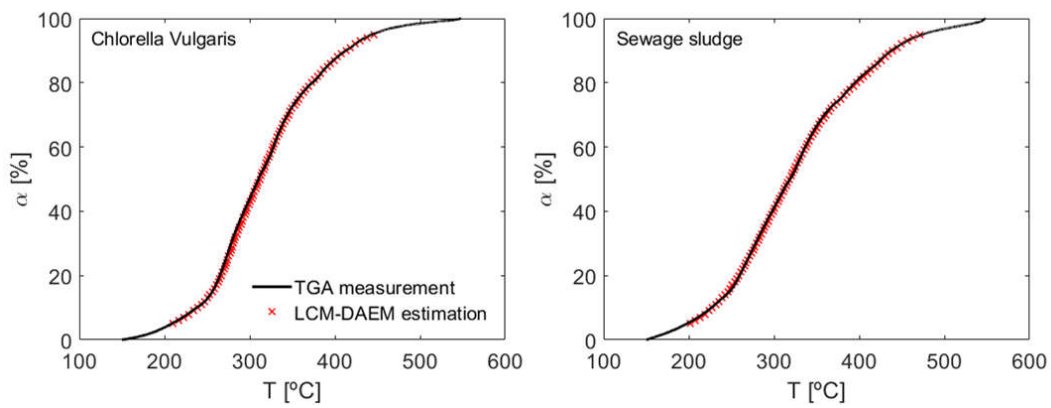


Figure 5. Comparison of the pyrolysis conversion of *Chlorella Vulgaris* and sewage sludge as a function of temperature experimentally measured in TGA and estimated by LCM-DAEM model for $T_\infty = 550 \text{ }^\circ\text{C}$ and $c = 0.06 \text{ min}^{-1}$.

The results of the comparison between LCM-DAEM model predictions and TGA measurements for the rest of cases, i.e., different reactor temperatures and heating parameters, are similar to those shown in Figure 5. The Root Mean Square Error (RMSE) was calculated for each case to quantify the deviation between the LCM-DAEM estimations and the TGA experimental measurements of temperature for each value of the pyrolysis conversion. These deviations of the proposed LCM-DAEM model from the experimental measurements, regarding the RMSE of temperature, are reported in Table 3 for the pyrolysis of both *Chlorella Vulgaris* and sewage sludge under the different reactor temperatures and heating parameters analyzed. The values obtained for the RMSE of temperature are lower than 5 °C in all cases, therefore, the proposed LCM-DAEM model was proven to accurately describe the pyrolysis of biomass under inverse exponential temperature increases, as those to which thermally small particles are subjected.

Table 3. Root Mean Square Error (RMSE) [°C] between temperature measured by TGA and estimated by the LCM-DAEM model for each value of the conversion between 5% and 95%.

	c = 0.06 min⁻¹		c = 0.18 min⁻¹	
	T_∞ = 550 °C	T_∞ = 650 °C	T_∞ = 550 °C	T_∞ = 650 °C
Chlorella Vulgaris	1.6	2.6	2.9	4.2
Sewage Sludge	1.5	3.8	2.3	4.7

The estimations of the proposed LCM-DAEM and the experimental pyrolysis measurements conducted in TGA were also compared in terms of the average

relative error of temperature for each value of the pyrolysis conversion between 5% and 95%. This relative error was defined as the temperature deviation between the model prediction and the experimental measurement divided by the experimental temperature. The values of the average relative error obtained in each case for both *Chlorella Vulgaris* and sewage sludge can be found in Table 4. An average relative error of temperature below 1% is obtained in all cases, confirming the accuracy of the proposed LCM-DAEM model.

Table 4. Average relative error [%] between temperatures measured by TGA and estimated by the LCM-DAEM model for each value of the conversion between 5% and 95%.

	$c = 0.06 \text{ min}^{-1}$		$c = 0.18 \text{ min}^{-1}$	
	$T_{\infty} = 550 \text{ }^{\circ}\text{C}$	$T_{\infty} = 650 \text{ }^{\circ}\text{C}$	$T_{\infty} = 550 \text{ }^{\circ}\text{C}$	$T_{\infty} = 650 \text{ }^{\circ}\text{C}$
Chlorella Vulgaris	0.24	0.36	0.46	0.64
Sewage Sludge	0.23	0.42	0.30	0.71

5. Conclusions

A simple model combining the LCM and the simplified DAEM was proposed to describe the pyrolysis process of thermally small biomass particles. The model is based on an Arrhenius equation accounting for both the inverse exponential temperature increase predicted by the LCM and the chemical kinetics described by the simplified DAEM. The Arrhenius equation on which the model is based was derived, for a variable reactor temperature, considering the pyrolysis chemical kinetics data of several lignocellulosic biomass samples. Solving this

simple Arrhenius equation, the evolution of the pyrolysis conversion of thermally small biomass particles subjected to a higher reactor temperature can be directly estimated.

The validation of the model was based on TGA measurements of the pyrolysis of *Chlorella Vulgaris* and sewage sludge under inverse exponential temperature profiles. The deviation between the LCM-DAEM model predictions and the TGA measurements for the relation between pyrolysis conversion and temperature, regarding the RMSE of temperature, is lower than 5 °C for all the cases tested. Concerning the average relative error between the temperatures estimated by the model and measured by the TGA, deviations below 1 % were obtained in all cases. Therefore, the proposed LCM-DAEM model was proven to accurately describe the evolution of the pyrolysis conversion with temperature for thermally small biomass particles. Furthermore, the difference in composition between the lignocellulosic samples, used to derive the Arrhenius equations, and the microalgae and sewage sludge, employed for the experimental measurements, guarantees the validity of the simple LCM-DAEM model proposed for a broad range of solid fuels, provided that the particle size is sufficiently small. Once the model was validated with TGA experimental measurements, it could be extended to consider also the dynamics of industrial pyrolysis reactors.

Acknowledgments

The authors express their gratitude to the BIOLAB experimental facility and to the “Programa de movilidad de investigadores en centros de investigación extranjeros (Modalidad A)” from the Carlos III University of Madrid (Spain) for the financial support conceded to Antonio Soria-Verdugo for a research stay at

the German Aerospace Center DLR (Stuttgart, Germany) during the summer of 2018. Funding by Deutsches Zentrum für Luft- und Raumfahrt e. V. (DLR), the German Aerospace Center, is also gratefully acknowledged.

References

Anca-Couce A. Reaction mechanisms and multi-scale modelling of lignocellulosic biomass pyrolysis. *Prog. Energ. Combust.* 2016; 53, 41-79.

Bach Q.V., Chen W.H. Pyrolysis characteristics and kinetics of microalgae via thermogravimetric analysis (TGA): A state-of-the-art review. *Bioresource Technol.* 2017; 246, 88-100.

Basu P. Biomass gasification and pyrolysis - Practical design and theory. Elsevier Inc.; 2010.

Bleistein N., Handelsman R.A. Asymptotic expansions of integrals, Dover Publications Inc, New York, 1987.

Cai J., Liu R. New distributed activation energy model: numerical solution and application to pyrolysis kinetics of some types of biomass. *Bioresource Technol.* 2008; 99, 2795-2799.

Cai J., Wu W., Liu R. An overview of distributed activation energy model and its application in the pyrolysis of lignocellulosic biomass. *Renew. Sust. Energ. Rev.* 2014; 36, 236-246.

Ceylan S., Kazan D. Pyrolysis kinetics and thermal characteristics of microalgae *Nannochloropsis oculata* and *Tetraselmis* sp. *Bioresource Technol.* 2015; 187, 1-5.

Coats A.W., Redfern J.P. Kinetic parameters from thermogravimetric data. *Nature*. 1964; 201, 68-69.

Czernik S., Bridgwater A.V. Overview of applications of biomass fast pyrolysis. *Oil. Energ. Fuel*. 2004; 18, 590-598.

Figueira C.A., Moreira P.F., Giudici R. Thermogravimetric analysis of the gasification of microalgae *Chlorella Vulgaris*. *Bioresource Technol*. 2015; 198, 717-724.

Günes M., Günes S.K. Distributed activation energy model parameters of some Turkish coals. *Energy Sources Part A* 2008; 30, 1460-1472.

Incropera F.P., De Witt D.P., Bergman T.L., Lavine A.S. *Fundamentals of heat and mass transfer*, 6th ed., John Wiley & Sons, United States of America, 2007.

Li Z., Zhao W., Meng B., Liu C., Zhu Q., Zhao G. Kinetic study of corn straw pyrolysis: comparison of two different three-pseudo component models. *Bioresource Technol*. 2008; 99, 7616-7622.

Lin T., Goos E., Riedel U. A sectional approach for biomass: Modelling the pyrolysis of cellulose. *Fuel Process. Technol*. 2013; 115, 246-253.

McKendry P. Energy production from biomass (part 2): conversion technologies. *Bioresource Technol*. 2002; 83, 47-54.

Miura K. A new and simple method to estimate $f(E)$ and $k_0(E)$ in the distributed activation energy model from three sets of experimental data. *Energ. Fuel*. 1995; 9, 302-307.

Miura K., Maki T. A simple method for estimating $f(E)$ and $k_0(E)$ in the distributed activation energy model. *Energ. Fuel.* 1998; 12, 864-869.

Pattara C., Cappelletti G.M., Cichelli A. Recovery and use of olive stones: Commodity, environmental and economic assessment. *Renew. Sust. Energ. Rev.* 2010; 14, 1484-1489.

Sharma A., Pareek V., Zhang D. Biomass pyrolysis - A review of modelling, process parameters and catalytic studies. *Renew. Sust. Energ. Rev.* 2015; 50, 1081-1096.

Sonobe T., Worasuwanarak N. Kinetic analyses of biomass pyrolysis using the distributed activation energy model. *Fuel* 2008; 87, 414-421.

Soria-Verdugo A., García-Hernando N., Garcia-Gutierrez L.M., Ruiz-Rivas U. Analysis of biomass and sewage sludge devolatilization using the distributed activation energy model. *Energ. Convers. Manage.* 2013; 65, 239-244.

Soria-Verdugo A., Garcia-Gutierrez L.M., Blanco-Cano L., Garcia-Hernando N., Ruiz-Rivas U. Evaluating the accuracy of the Distributed Activation Energy Model for biomass devolatilization curves obtained at high heating rates. *Energ. Convers. Manage.* 2014; 86 1045-1049.

Soria-Verdugo A., Goos E., García-Hernando N. Effect of the number of TGA curves employed on the biomass pyrolysis kinetics results obtained using the Distributed Activation Energy Model. *Fuel Process. Technol.* 2015; 134, 360-371.

Soria-Verdugo A., Goos E., Arrieta-Sanagustín J., García-Hernando N. Modeling of the pyrolysis of biomass under parabolic and exponential

temperature increases using the Distributed Activation Energy Model. *Energ. Convers. Manage.* 2016; 118, 223-230.

Soria-Verdugo A., Morato-Godino A., Garcia-Gutierrez L.M., García-Hernando N. Pyrolysis of sewage sludge in a fixed and a bubbling fluidized bed – Estimation and experimental validation of the pyrolysis time. *Energ. Convers. Manage.* 2017a; 144, 235-242.

Soria-Verdugo A., Goos E., Morato-Godino A., García-Hernando N., Riedel U. Pyrolysis of biofuels of the future: Sewage sludge and microalgae - Thermogravimetric analysis and modelling of the pyrolysis under different temperature conditions. *Energ. Convers. Manage.* 2017b; 138, 261-272.

Soria-Verdugo A., Goos E., García-Hernando N., Riedel U. Analyzing the pyrolysis kinetics of several microalgae species by various differential and integral isoconversional kinetic methods and the Distributed Activation Energy Model. *Algal Res.* 2018; 32, 11-29.

Vand V. A theory of the irreversible electrical resistance changes of metallic films evaporated in vacuum. *Proc. Phys. Soc.* 1943; 55, 222-246.

Várghegyi G., Szabó P., Antal M.J. Kinetics of charcoal devolatilization. *Energ. Fuel* 2002; 16, 724-731.

Vyazovkin S.V., Lesnicovich A.I. Practical application of isoconversional methods. *Thermochim. Acta.* 1992; 203, 177-185.

Wang Q., Wang H., Sun B., Bai J., Guan X. Interactions between oil shale and its semicoke during co-combustion. *Fuel* 2009; 88, 1520-1529.

WanJun T., Cunxin W., Donghua C. Kinetic studies on the pyrolysis of chitin and Chitosan. *Polym. Degrad. Stab.* 2005; 87, 389-394.

Yan J.H., Zhu H.M., Jiang X.G., Chi Y., Cen K.F. Analysis of volatile species kinetics during typical medical waste materials pyrolysis using a distributed activation energy model. *J. Hazard. Mater.* 2009; 162, 646-651.

List of figures

Figure 1. Process to determine ϕ_{ie} .

Figure 2. Values obtained for ϕ_{ie} as a function of the reactor temperature T_{∞} (black +) and parabolic fitting (red dashed line).

Figure 3. Temperature profiles measured in the TGA for different reactor temperatures and heating parameters.

Figure 4. Pyrolysis conversion curves for Chlorella Vulgaris and sewage sludge.

Figure 5. Comparison of the pyrolysis conversion of Chlorella Vulgaris and sewage sludge as a function of temperature experimentally measured in TGA and estimated by LCM-DAEM model for $T_{\infty} = 550$ °C and $c = 0.06$ min⁻¹.

List of tables

Table 1. Pyrolysis kinetic data of various lignocellulosic biomass species.

Table 2. Results of the basic characterization of *Chlorella Vulgaris* and sewage sludge (PA: Proximate Analysis, UA: Ultimate Analysis, VM: Volatile Matter, A: Ash, C: Carbon, H: Hydrogen, N: Nitrogen, S: Sulfur, O: Oxygen, HHV: High Heating Value, db: dry basis, daf: dried ash free basis, * calculated by difference).

Table 3. Root Mean Square Error (RMSE) [$^{\circ}\text{C}$] between temperature measured by TGA and estimated by the LCM-DAEM model for each value of the conversion between 5% and 95%.

Table 4. Average relative error [%] between temperatures measured by TGA and estimated by the LCM-DAEM model for each value of the conversion between 5% and 95%.